

# Patterns of Fundus Autofluorescence Lifetimes In Eyes of Individuals With Nonexudative Age-Related Macular Degeneration

Lydia Sauer,<sup>1,2</sup> Rebekah H. Gensure,<sup>1</sup> Karl M. Andersen,<sup>1,3</sup> Lukas Kreilkamp,<sup>2</sup> Gregory S. Hageman,<sup>1,4</sup> Martin Hammer,<sup>2</sup> and Paul S. Bernstein<sup>1</sup>

<sup>1</sup>Department of Ophthalmology and Visual Sciences, John A. Moran Eye Center, University of Utah, Salt Lake City, Utah, United States

<sup>2</sup>Department of Experimental Ophthalmology, University Hospital Jena, Jena, Germany

<sup>3</sup>Geisinger Commonwealth School of Medicine, Scranton, Pennsylvania, United States

<sup>4</sup>Sharon Eccles Steele Center for Translational Medicine, John A. Moran Eye Center, University of Utah, Salt Lake City, Utah, United States

Correspondence: Paul S. Bernstein, John A. Moran Eye Center, University of Utah, 65 Mario Capecchi Drive, Salt Lake City, UT 84132, USA; paul.bernstein@hsc.utah.edu.

Submitted: January 1, 2018

Accepted: May 11, 2018

Citation: Sauer L, Gensure RH, Andersen KM, et al. Patterns of fundus autofluorescence lifetimes in eyes of individuals with nonexudative age-related macular degeneration. *Invest Ophthalmol Vis Sci.* 2018;59:AMD65-AMD77. <https://doi.org/10.1167/iov.17-23764>

**PURPOSE.** To investigate fundus autofluorescence (FAF) lifetimes in patients with nonexudative AMD.

**METHODS.** A total of 150 eyes of 110 patients (mean age:  $73.2 \pm 10.7$  years) with nonexudative AMD, as well as a healthy group of 57 eyes in 38 subjects (mean age:  $66.5 \pm 8.7$  years), were included. Investigations were conducted at the University Eye Clinic in Jena, Germany, as well as the Moran Eye Center in Salt Lake City, Utah, USA, using the Heidelberg Engineering Spectralis-based fluorescence lifetime imaging ophthalmoscope (FLIO). A 30° retinal field centered at the fovea was investigated. FAF decays were detected in short (498–560 nm) and long (560–720 nm, LSC) spectral channels. The mean fluorescence lifetimes ( $\tau_m$ ) were calculated. Optical coherence tomography scans and fundus photographs were also recorded.

**RESULTS.** In patients with nonexudative AMD, FLIO shows a ring-shaped pattern of prolonged  $\tau_m$  in the LSC. This pattern occurs in all patients with AMD (including very early stages) and in one-third of the healthy controls. FAF lifetimes were longer with more advanced stages. The presence of drusen is associated with prolonged  $\tau_m$  when compared with the healthy fundus, but drusen identification is difficult with FLIO only.

**CONCLUSIONS.** FLIO detects a clear pattern of changes within the fundus, which appears to be AMD-associated. These changes are already visible in early AMD stages and not masked by the presence of other coexisting retinal diseases. These findings may be useful for the early diagnosis of AMD and to distinguish AMD from other retinal diseases.

**Keywords:** FLIO, fluorescence lifetime imaging, AMD, lipofuscin

AMD is a major cause of vision loss in individuals older than 65 years.<sup>1,2</sup> The number of affected individuals is still rising, due to the aging of the population.<sup>3</sup> Genetic risk, as well as environment, are involved in AMD pathogenesis.<sup>4–7</sup> Whereas exudative AMD can be treated with injections of anti-VEGF antibodies and antibody fragments, no treatment is available for nonexudative, early-stage AMD.<sup>1,3</sup> A protective benefit of carotenoid supplementation has been discussed.<sup>8,9</sup> Drusen, the hallmark pathological feature of AMD, are extracellular debris deposits located between the basal lamina of the RPE and Bruch membrane's inner collagenous layer.<sup>4,10</sup> Chronic inflammation caused by cellular remnants and debris, as well as complement dysregulation, seem to play a role in their development.<sup>11–13</sup> Currently, nonexudative AMD is clinically diagnosed according to drusen and pigment changes identified on fundus examination as well as optical coherence tomography (OCT) and autofluorescence findings.

Early detection of AMD may provide opportunity to intervene with supplementation and may thus result in a better visual outcome with preserved central visual acuity. In many

cases, the initial clinical diagnosis of AMD is correct. However, accumulation of a variety of types of material may also occur in diseases other than AMD.<sup>14</sup> Such diseases may be misdiagnosed as AMD due to the similar appearance between these drusen-like deposits and true AMD drusen. Additionally, various diseases may cause retinal changes and may therefore also be misdiagnosed as the very common AMD. An accurate determination would be helpful for cases of early-onset drusen, which are not related to AMD. Additionally, AMD should be distinguished from other retinal diseases with similar appearance.

Fluorescence lifetime imaging ophthalmoscopy (FLIO) is a novel method to investigate metabolic and disease-related changes within the retina.<sup>15–17</sup> Measurements based on fluorescence lifetime imaging are very sensitive and may pick up small environmental changes at the human fundus. In the same manner, the investigation procedure should be conducted carefully and consistently. In addition to conventional fundus autofluorescence (FAF) intensity imaging, FLIO also detects the fluorescence decay over time at each pixel, which is known as



the FAF lifetime. According to the retinal status (healthy or otherwise), FLIO has been shown to exhibit different FAF lifetime patterns. Patterns of healthy eyes have been thoroughly investigated in previous studies.<sup>18–20</sup> Changes in FAF lifetimes also have been described in other disease states, such as macular holes, Stargardt disease, diabetic retinopathy, central serous chorioretinopathy, macular telangiectasia type 2, retinitis pigmentosa, and AMD-associated geographic atrophy (GA).<sup>21–28</sup> Retinal drusen in AMD were recently investigated with FLIO.<sup>29</sup> In that study, drusen were staged according to their size and divided into soft drusen and reticular pseudo-drusen based on their appearance on OCT and infrared images. Dysli and colleagues<sup>29</sup> found a general prolongation of FAF lifetimes and variable FAF lifetime characteristics in drusen. Time-resolved FAF also has been described for drusen in donor tissue previously.<sup>30</sup>

The present study shows *in vivo* imaging results of patients affected with AMD and focuses on early and intermediate stages. Previously, a general prolongation of FAF lifetimes in AMD was described. In the current study, we find that these prolongations appear in a specific FAF lifetime pattern in all eyes affected with early- and intermediate-stage AMD and in one-third of the healthy controls. This pattern is likely disease-associated. In addition, characteristics of different drusen types are investigated.

## METHODS

This cross-sectional study was conducted at the Department of Ophthalmology at the University Hospital in Jena, Germany, and the John A. Moran Eye Center of the University of Utah in Salt Lake City, Utah, United States. It was approved by a local ethics committee in Jena and by the University of Utah Institutional Review Board. This study adhered to the Declaration of Helsinki. Informed written consent was obtained from all patients before any investigations. All measurements in Jena were performed between April 2014 and April 2016 at the University Hospital in Jena. The measurements in Salt Lake City were performed between March and June 2017 at the Moran Eye Center in Salt Lake City, Utah, United States.

### Procedure

All patients were examined by an ophthalmologist and diagnosed with nonexudative AMD before inclusion. Eyes with a history of exudative AMD were excluded. Best corrected visual acuity was obtained, and pupils were dilated. Each underwent an FLIO measurement, and all but the healthy subjects also received an OCT scan (Jena: Zeiss Cirrus, Meditec AG, Jena, Germany; Salt Lake City: Heidelberg Engineering Spectralis, Heidelberg, Germany) as well as fundus photography. Fluorescein was not used when assessing IOP, and all study procedures were completed before performance of any fluorescein angiography procedures.

AMD was classified according to the Beckman Initiative for Macular Research Classification Committee as early (medium drusen, 63 to <125  $\mu\text{m}$ ), intermediate (drusen >125  $\mu\text{m}$ , pigmentary changes) and late (GA) AMD.<sup>31</sup> Different drusen types, including hard, soft, and reticular pseudodrusen were classified with OCT, fundus photography, and infrared imaging.

### Fluorescence Lifetime Imaging Ophthalmoscopy

The FLIO device setup, safety, and image acquisition have been previously described in detail.<sup>17–19,24</sup> Briefly, the prototype FLIO is based on a Heidelberg Engineering Spectralis and

records FAF lifetimes *in vivo* relying on the principle of time-correlated single-photon counting.<sup>17,32</sup> Two different FLIO devices were used at the two different institutions. FAF lifetime and intensity images were acquired from a 30° field centered at the fovea (excitation wavelength 473 nm). Photons were detected in two separate spectral channels: a short spectral channel (SSC; 498 to 560 nm) and a long spectral channel (LSC; 560 to 720 nm). A high-contrast confocal infrared reflectance image for eye tracking was included.

Fluorescence data were analyzed using the software SPCImage 4.4.2 (Becker & Hickl GmbH, Berlin, Germany). The fluorescence decay was approximated by calculating the least-square fit of a series of three exponential functions; 3 × 3-pixel binning was applied. The amplitude weighted mean fluorescence decay time ( $\tau_m$ ) was used for further analysis. Further details may be found elsewhere.<sup>18,32</sup>

FAF lifetimes showed significant differences between both devices, as the Jena device presents shorter FAF lifetimes. This is caused by the different calibration of the devices. Nevertheless, even with these differences, both devices showed comparable results with regard to the pattern described below. Therefore, a multicentered study is possible.

SPCImage and FLIMX were used to illustrate the FAF lifetimes.<sup>33</sup> The FLIMX software is documented and freely available for download online under the open source BSD-license (in the public domain, <http://www.flimx.de>).

All drusen masks were generated according to a combination of the FAF intensity image and fundus photograph. They were marked in the FAF intensity image, which uses the same cursor as the FAF lifetime image in the SPCImage software.

### Statistical Analysis

SPSS 21 (SPSS, Inc., Chicago, IL, USA) was used in all statistical analyses. To test for significant  $\tau_m$  differences between regions in one eye, a *t*-test for paired samples was used. To compare hard drusen with soft drusen, a *t*-test for independent samples was used. Our data followed normal distribution (checked with the Kolmogorov-Smirnov test), and all results are provided as mean  $\pm$  SD.

## RESULTS

### Subjects

This study included a total of 150 eyes from 110 patients with nonexudative AMD without prior evidence of progression to exudative AMD. The mean age over all patients was 73.2  $\pm$  10.7 years. Of particular interest were early and intermediate AMD stages, with 104 of the investigated AMD eyes (mean age: 71.8  $\pm$  10.3 years); 40 (39%) of the investigated early/intermediate AMD eyes were pseudophakic. A total of 57 healthy eyes also were included and compared with the eyes with early and intermediate AMD. The mean age of these controls was 66.5  $\pm$  8.7 years. A detailed characterization of all subjects is given in Table 1.

Patients with late AMD (GA, 30 eyes) as well as eyes with AMD and other diseases (AMD and macular telangiectasia type 2 [MacTel]: 8 eyes; AMD and macular hole: 3 eyes) were investigated to check for the AMD-specific pattern (as mentioned below). These eyes were not included in any statistical analyses.

### FLIO Pattern in Eyes With AMD

FAF lifetimes in AMD show a characteristic pattern of prolonged mean fluorescence decays when looking at the

TABLE 1. Characterization of Investigated Subjects

	Healthy		AMD	
	Jena	Salt Lake City	Jena	Salt Lake City
Number of eyes	12	45	32	72
Number of subjects	12	26	32	44
Mean age, y, ± SD	67.0 ± 8.0	66.2 ± 9.1	70.4 ± 7.6	72.0 ± 11.9
IOL, no. eyes (%)	5 (42)	14 (31)	12 (38)	28 (39)
Sex, F/M, n (%)	8 (67)/4 (33)	13 (50)/13 (50)	19 (59)/13 (41)	26 (59)/18 (41)
Early AMD, no. eyes (%)			7 (22)	27 (38)
Intermediate AMD, no. eyes (%)			25 (78)	45 (62)
<b>Number of eyes</b>		<b>57</b>		<b>104</b>
<b>Mean age, y, ± SD</b>		<b>66.5 ± 8.7</b>		<b>71.8 ± 10.3</b>
Additional eyes			Jena	Salt Lake City
Late AMD, no. eyes (mean age, y, ± SD)			19 (79.2 ± 6.0)	16 (82.6 ± 7.0)
MacTel + AMD, no. eyes (mean age, y, ± SD)			0	8 (66.5 ± 8.2)
Macular hole + AMD, no. eyes (mean age, y)			2 (68)	1 (79)
Total				
Number of eyes		57, 38 subjects		150, 110 patients
Mean age, y, ± SD		66.5 ± 8.7		73.2 ± 10.7

Bold shows the number of eyes used for statistical analysis.

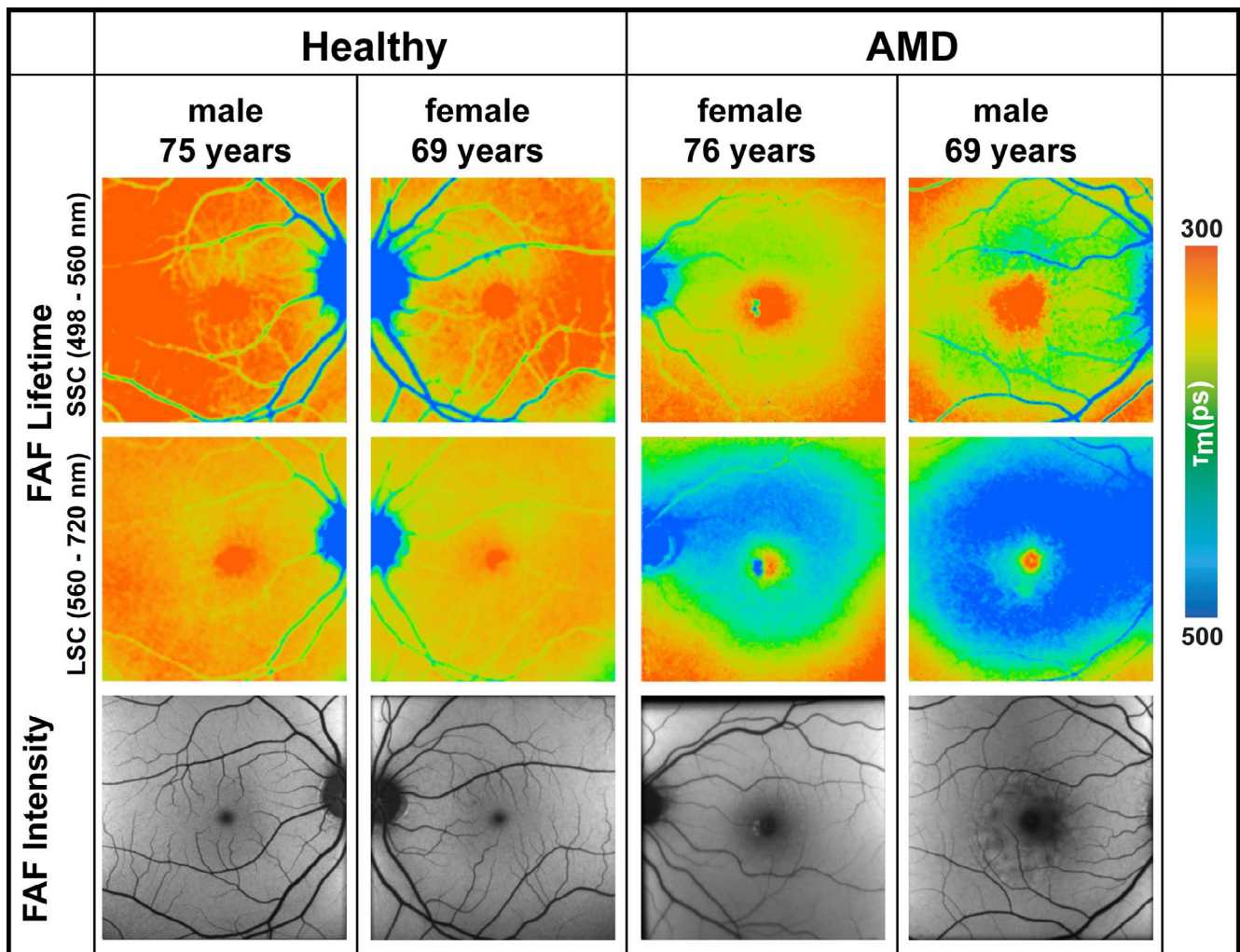


FIGURE 1. FAF lifetime images from the short (498–560 nm, SSC) and the long (560–720 nm, LSC) spectral channel as well as FAF intensity images of two healthy eyes and two eyes with nonexudative AMD.

TABLE 2. Mean FAF Lifetimes in Healthy Subjects and AMD Patients

Both Centers	Healthy, 57 Eyes	AMD, 104 Eyes	P	Mean Difference
C area, ps				
SSC	210 ± 77	196 ± 111	0.39	14 ± 17
LSC	284 ± 76	299 ± 100	0.29	15 ± 14
OR, ps				
SSC	313 ± 79	342 ± 124	0.08	29 ± 16
LSC	340 ± 71	403 ± 98	<0.001	63 ± 14
Difference, OR – C, ps				
SSC	103 ± 30	147 ± 46	<0.001	43 ± 6
LSC	56 ± 27	103 ± 46	<0.001	48 ± 6
Salt Lake City	Healthy, 45 Eyes	AMD, 72 Eyes	P	Mean Difference
C area, ps				
SSC	223 ± 80	228 ± 112	0.8	5 ± 19
LSC	309 ± 66	339 ± 81	0.06	30 ± 15
OR, ps				
SSC	327 ± 80	380 ± 120	<0.01	53 ± 19
LSC	361 ± 63	441 ± 83	<0.001	79 ± 14
Difference, OR – C, ps				
SSC	104 ± 26	152 ± 49	<0.001	48 ± 7
LSC	53 ± 26	101 ± 51	<0.001	49 ± 7
Jena	Healthy, 12 Eyes	AMD, 32 Eyes	P	Mean Difference
C area, ps				
SSC	162 ± 44	123 ± 64	0.06	38 ± 20
LSC	195 ± 32	209 ± 80	0.41	14 ± 17
OR, ps				
SSC	263 ± 49	257 ± 87	0.83	6 ± 26
LSC	262 ± 38	317 ± 72	<0.05	55 ± 22
Difference, OR – C, ps				
SSC	102 ± 44	135 ± 36	<0.05	33 ± 13
LSC	67 ± 27	108 ± 34	<0.001	41 ± 9

LSC. It is ring-shaped and presents between the large vessels with a diameter approximately 3 mm to 6 mm centered at the fovea (Fig. 1). Placing a standardized Early Treatment Diabetic Retinopathy Study (ETDRS) grid on the FLIO images, the AMD-related pattern fits the area of the outer ring. This pattern is usually visible if the pseudo-color range of  $\tau_m$  is set from 300 to 500 ps in the software. As strong cataracts were an exclusion criterion in this study, no further investigations were done on these eyes. The color range might be different for these cases. In the SSC, the typical pattern was found in some patients with more advanced AMD. However, not every eye with AMD showed such typical and obvious changes within the SSC. Therefore, this study focuses on the LSC.

Similar to healthy eyes, eyes with AMD show longest  $\tau_m$  at the optic nerve head and shortest  $\tau_m$  within the fovea. The pattern at the rest of the retina in AMD differs from healthy eyes. Whereas healthy eyes show a homogeneous distribution of intermediate-long FAF decays across the retina in the LSC, eyes affected with AMD show a ring-shaped prolongation of  $\tau_m$  between the vessel arcade in the macular region, which is shown in Figure 1. This figure presents FAF lifetimes for two typical eyes with early- and intermediate-stage AMD as well as two healthy eyes. As the figure illustrates, the area of prolonged  $\tau_m$  measurements nearly fills the entire space between the arcades while sparing the fovea. Figure 2 shows FAF lifetimes from the LSC of additional AMD eyes with this pattern.

The area exhibiting this pattern corresponds to the outer ring (OR) from a standardized ETDRS grid. Figure 3A depicts the OR, as well as other regions of interest (ROIs). Investigations conducted across all early and intermediate AMD eyes (both clinical sites) showed foveal  $\tau_m$  (ROI: central area [C]) that were significantly shorter than  $\tau_m$  of the OR in both spectral channels ( $P < 0.001$ ) (Table 2). In the case of drusen within the foveal region, foveal  $\tau_m$  appeared prolonged, but in mean still shorter than at the OR. The differences in FAF lifetimes between the OR and the foveal center were  $147 \pm 46$  ps (LSC) and  $103 \pm 46$  ps (LSC).

By further dividing the OR into four regions, the pattern was most prominent at the superior-nasal side. Here, the longest decay constants were observed ( $\tau_m$  for regions superior [S]:  $417 \pm 99$  ps; nasal [N]:  $419 \pm 103$  ps; temporal [T]:  $382 \pm 96$  ps; inferior [I]:  $390 \pm 99$  ps).  $\tau_m$  in S and N regions were significantly longer than in T and I regions ( $P < 0.05$ ). No significant differences were found when comparing S with N ( $P = 0.94$ ) and T with I ( $P = 0.56$ ). Figure 3B shows this.

### AMD Compared With Healthy Eyes

FAF lifetimes from eyes with AMD were compared with healthy eyes. Mean FAF decays of the foveal ROI (area C) as well as the pattern-related ROI of the OR were hereby investigated. The FAF lifetimes of the ROIs in healthy as well as AMD eyes are highlighted in form of a boxplot in Figure 3C. Table 2 depicts FAF lifetime differences of healthy eyes as compared with AMD eyes across the different ROIs for both spectral channels. At the fovea, no significant difference was found between healthy and AMD eyes.  $\tau_m$  in the ROI of the OR, however, did show significant differences between those groups (LSC:  $P < 0.001$ ). Age-matched healthy eyes showed significantly shorter FAF lifetimes at the OR as compared with AMD eyes.

Additional to the investigation of all eyes, the two study sites were also investigated separately. In the smaller Jena cohort, significances were less strong ( $P < 0.05$ ). Comparing the FAF lifetimes from both study sites, lifetimes from area C and the ROI of the OR are significantly shorter in Jena. As mentioned within the Methods section, this is due to a different calibration method. However, when looking at differences between these regions, we did not find any significant difference between the two study sites. Patterns in AMD can be seen similarly in patients from both sites. Nevertheless, to conduct a clean analysis, all further subgroup statistical analyses are presented only on measurements from the Moran Eye Center.

Setting the color range to 300 to 500 ps within the group of presumably healthy eyes from Utah, 6 eyes (mean age: 64 years) showed the same pattern and an additional 10 eyes (mean age: 68.7 years) showed the pattern in a less intense form (trace pattern). In total, 36% of our healthy individuals from Utah showed the pattern. Of these eyes, however, eight eyes also showed a few small drusen ( $<63 \mu\text{m}$ ) but no further signs of AMD. A positive family history of AMD was very common in these patients. Figure 4 shows the less intense pattern in a healthy eye, as well as trace pattern. No pattern was found in 41 (64%) of the presumably healthy eyes (mean age: 65.2 years).

FAF lifetimes from the main ROI of the OR (LSC) were obtained from patients as well as healthy subjects (both from the Utah cohort) and analyzed according to the presence of the pattern. Figure 5A shows how FAF lifetimes from this ROI differ between groups. We found significant differences between healthy eyes with and without the pattern ( $P < 0.05$ ). There also were significant differences between healthy eyes without pattern and AMD eyes ( $P <$

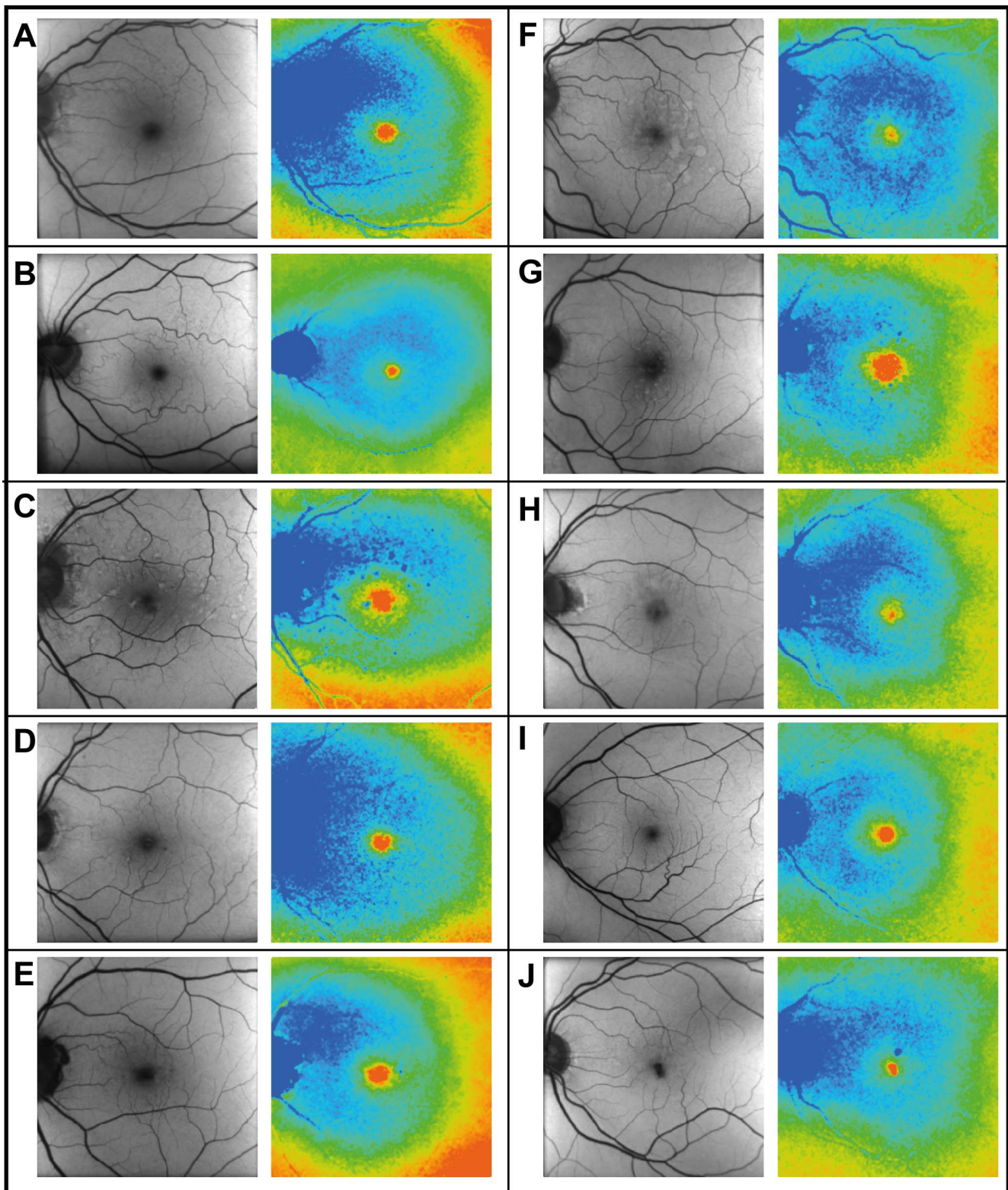


**FIGURE 2.** Mean FAF lifetimes (LSC) of 10 different patients with AMD showing the AMD-related pattern. Patient characteristics (y, year-old; m, male; f, female): (A) f, 72 y; (B) f, 69 y; (C) m, 66 y; (D) m, 87 y; (E) f, 79 y; (F) m, 72 y; (G) m, 77 y; (H) m, 86 y; (I) f, 72 y; (J) f, 73 y.

0.001). However, no significant difference was found between healthy eyes with the pattern and AMD eyes. We further investigated these differences within the healthy eyes. Eyes with only trace pattern did not show significant

differences to eyes without the pattern. However, eyes with a strong pattern showed significantly different FAF lifetimes in the ROI of the OR than the other groups ( $P < 0.01$ ). Figure 5B depicts this finding.

TABLE 3. Mean FAF Lifetimes in Different AMD Stages

	Early AMD	Intermediate AMD	P	Mean Difference
C area, ps				
SSC	214 ± 72	236 ± 131	0.43	22 ± 27
LSC	331 ± 80	344 ± 82	0.49	14 ± 19
OR, ps				
SSC	347 ± 82	400 ± 134	<0.05	53 ± 26
LSC	416 ± 86	456 ± 78	<0.05	40 ± 20
Difference, OR – C, ps				
SSC	133 ± 28	164 ± 55	<0.01	31 ± 10
LSC	85 ± 34	111 ± 57	<0.05	26 ± 11

**FAF Lifetimes in Different Disease Stages**

We investigated all AMD stages in this study. Figure 5C focuses on differences between early and intermediate AMD stages in the Utah cohort. Table 3 shows the corresponding FAF lifetime

differences between AMD stages. In the ROI of the OR, intermediate AMD (456 ± 78 ps) shows significantly more prolonged FAF lifetimes ( $P < 0.05$ ) than early AMD (416 ± 86 ps).

As late AMD has previously been investigated, we here simply focus on describing the AMD pattern in late-stage AMD. The 35 investigated eyes with late AMD (GA) also showed the pattern of prolonged FAF lifetimes. Similar to early and intermediate AMD, the color has to be adjusted (300 to 500, as described above). If done so, the pattern appears surrounding the area of atrophy. Figure 6A shows this finding and depicts a representative eye with GA. In these late AMD stages, the pattern appears most prominent of all investigated eyes. Due to atrophic processes in the areas of interest, which extremely prolong FAF lifetimes, no statistical analysis was conducted for these eyes.

**AMD Combined With Other Diseases**

The typical AMD pattern most prominently presents in the LSC, whereas other concurrent diseases, such as MacTel or

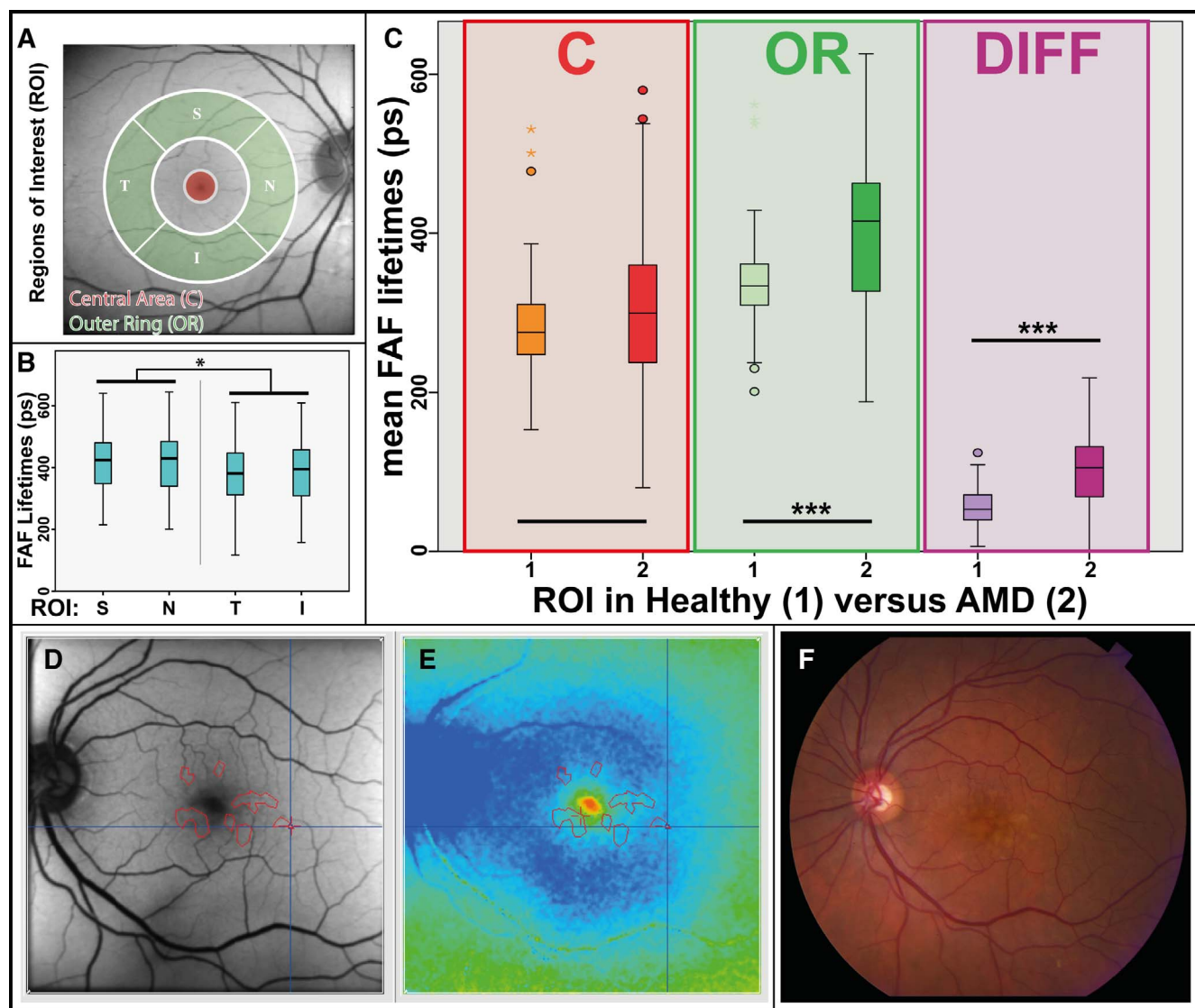


FIGURE 3. (A) ROIs demonstrated on an FAF intensity image from a representative patient with AMD: area C and OR. (B) Boxplot showing significant differences between S, N, T, and I regions of the OR ROI. No significant difference was found between S-N and T-I; all other regions were significantly different from each other.  $*P < 0.05$ . (C) Boxplot showing mean FAF lifetimes from ROIs (C, OR) in healthy eyes and AMD as well as the difference (OR minus C; Diff) for both groups.  $***P < 0.001$ . (D–F) Creation of masks for drusen in FAF lifetime image (E) based on FAF intensity image (D) and fundus photo (F). FAF lifetime and intensity images use the same cursor.

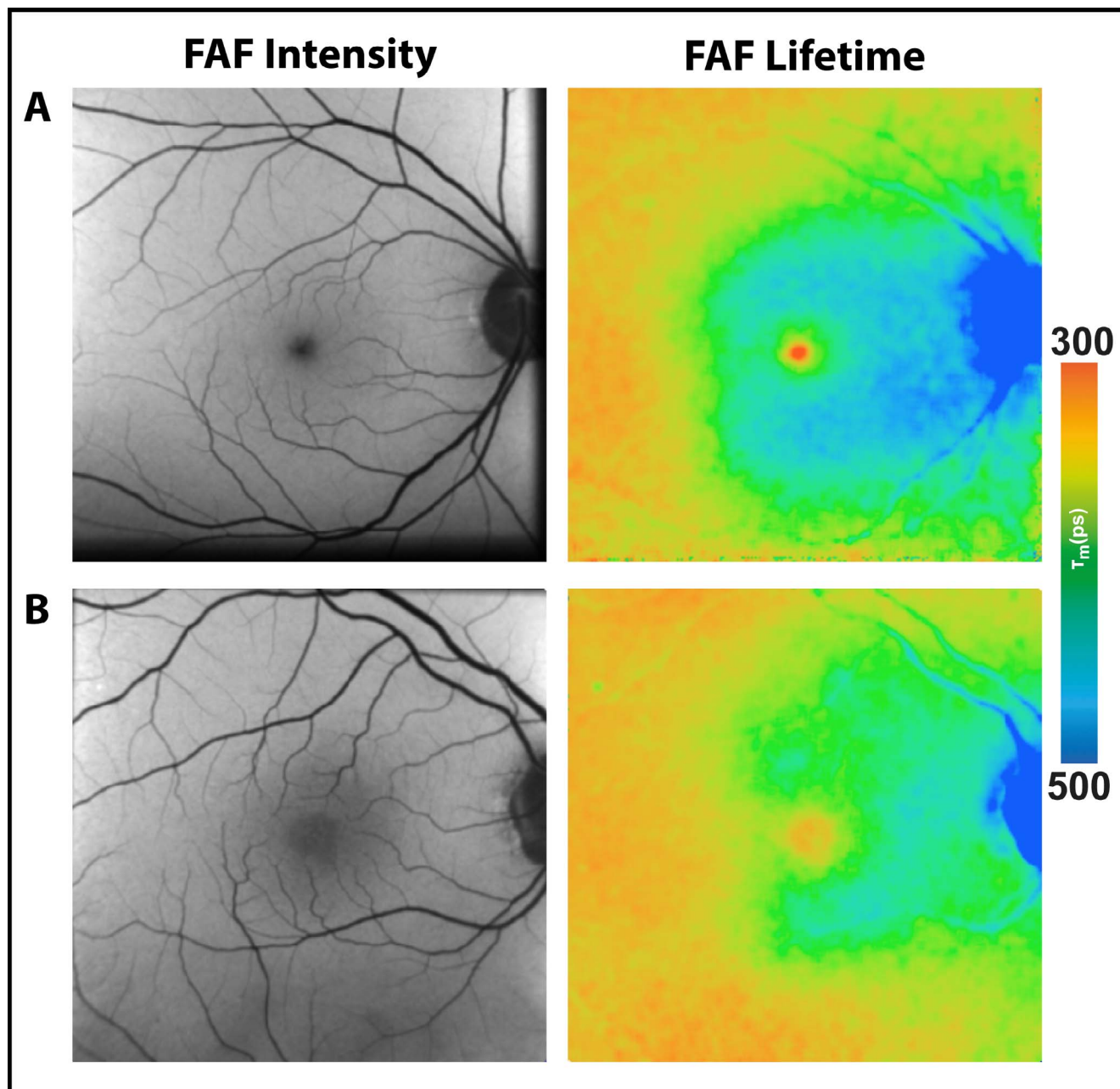


FIGURE 4. FAF intensity and lifetime (FLIO) images from the LSC (560–720 nm) of two healthy subjects with the AMD-related pattern: (A) subject with a less intense pattern (f, 61 y), and (B) subject with a trace pattern (f, 67 y).

macular holes, are easier to see in the SSC. Figures 6B through 6D show these findings for MacTel. Eyes with AMD show the typical signature in the LSC (Fig. 6B). Eyes with MacTel show a different, characteristic signature in the SSC (Fig. 6C). Eyes affected with both diseases show both patterns (Fig. 6D). The same applies for macular holes (no image shown).

#### FAF Lifetimes of Drusen

Figure 7 illustrates the AMD pattern of  $\tau_m$  in three different representative patients. Patient A has hard drusen; patient B has soft drusen, and patient C has reticular pseudodrusen. The fluorescence lifetimes of the macular region are prolonged for each of these patients within the LSC compared with non-AMD individuals.

The FAF lifetimes of drusen were analyzed within all AMD eyes investigated at the Moran Eye Center. Eyes with only one type of drusen (hard, soft, or pseudodrusen) were included in the analysis. In total, 60 of the 72 eyes investigated in Utah matched these criteria. In these eyes from the Utah recruitment group, 17 (28%) showed hard drusen (63–125  $\mu\text{m}$ ), 33 (55%) showed soft drusen (>125  $\mu\text{m}$ ), and 10 (17%) showed pseudodrusen. Masks of regions containing drusen were manually outlined for each of these subjects as described in the Methods section and presented in Figures 3D through 3F. A mask of retinal regions without drusen was generated for each subject similarly, finding drusen-free areas between the large vessels. Drusen are often difficult to observe in FLIO images, as shown in Figure 7. Whereas the FLIO study subject depicted in Figure 7A shows an obvious prolongation within the hard

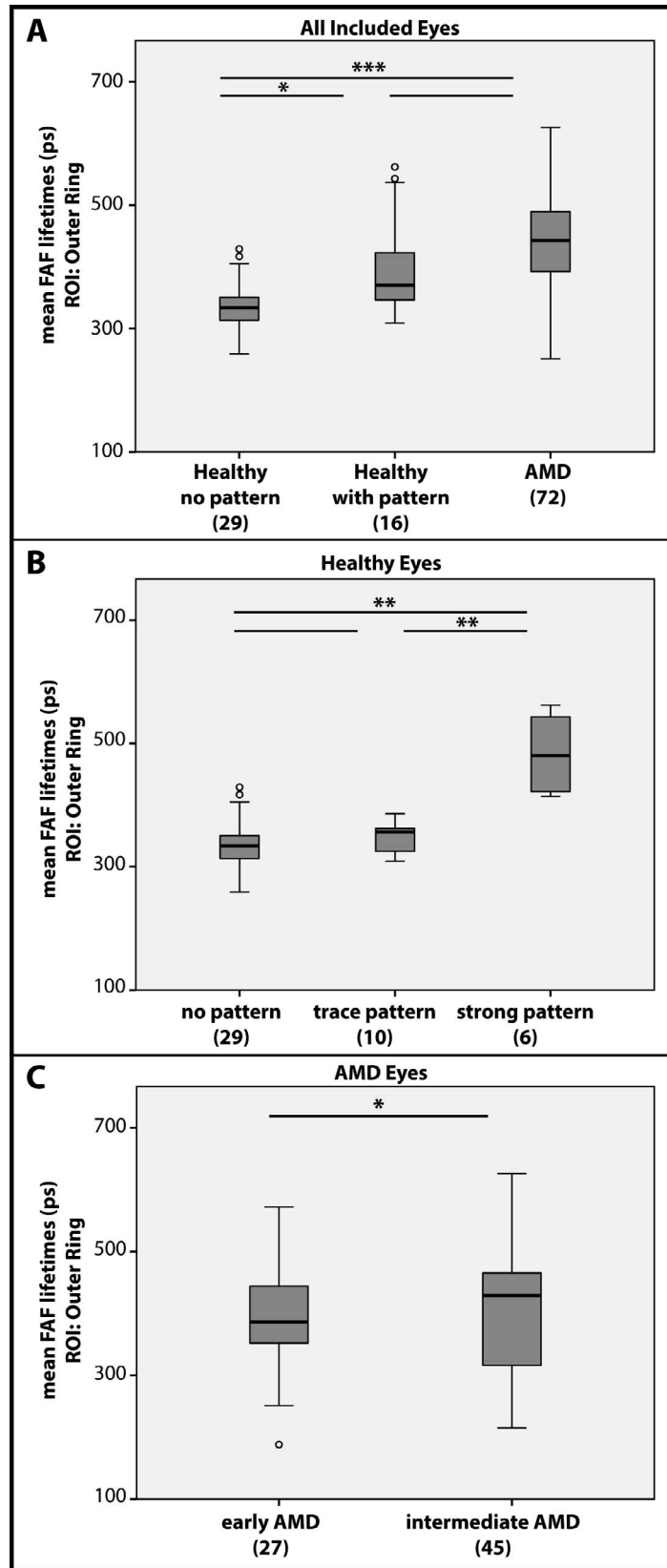


**FIGURE 5.** Mean FAF lifetimes from the ROI of the OR from the LSC. **(A)** All included eyes compared with regard to their pattern/disease status. **(B)** All healthy eyes compared with regard to their pattern. **(C)** AMD eyes compared with regard to the stage of the disease. \* $P < 0.05$ , \*\* $P < 0.01$ , \*\*\* $P < 0.001$ .



TABLE 4. Mean FAF Lifetimes in Drusen

Type	Channel	Drusen	Adjacent Retina	Mean Difference	Test	P
Hard, ps	SSC	356 ± 118	312 ± 92	44 ± 36	PS	<0.01
	LSC	416 ± 86	370 ± 66	46 ± 26	I	0.235
Soft, ps	SSC	421 ± 145	392 ± 144	29 ± 36	PS	<0.001
	LSC	474 ± 71	421 ± 72	53 ± 18	I	0.089
Pseudo, ps	SSC	362 ± 87	320 ± 77	42 ± 37	PS	<0.001
	LSC	468 ± 102	405 ± 87	62 ± 43	I	<0.01

I, independent t-test; PS, paired-sample t-test.

drusen, the soft drusen in Figure 7B are less apparent on the FLIO image. Reticular pseudodrusen are visibly prolonged in FAF lifetimes. However, the described ring pattern is often more obvious than the drusen themselves. Drusen in dry AMD mostly showed longer or similar FAF decays as compared to the retina without drusen. Spots of short FAF lifetimes in the LSC tended to appear in exudative AMD (data not shown, as this article focuses on nonexudative AMD only).

Mean FAF lifetimes of each drusen type can be found in Table 4. We performed a paired-sample t-test to individually compare different lifetimes in the different patients. Including all 60 patients, regardless of their drusen type, we found that drusen showed significantly longer FAF lifetimes as compared with the retina without drusen ( $P < 0.001$  in both spectral channels). Individually comparing each drusen type, all types showed significantly longer FAF lifetimes as compared with the

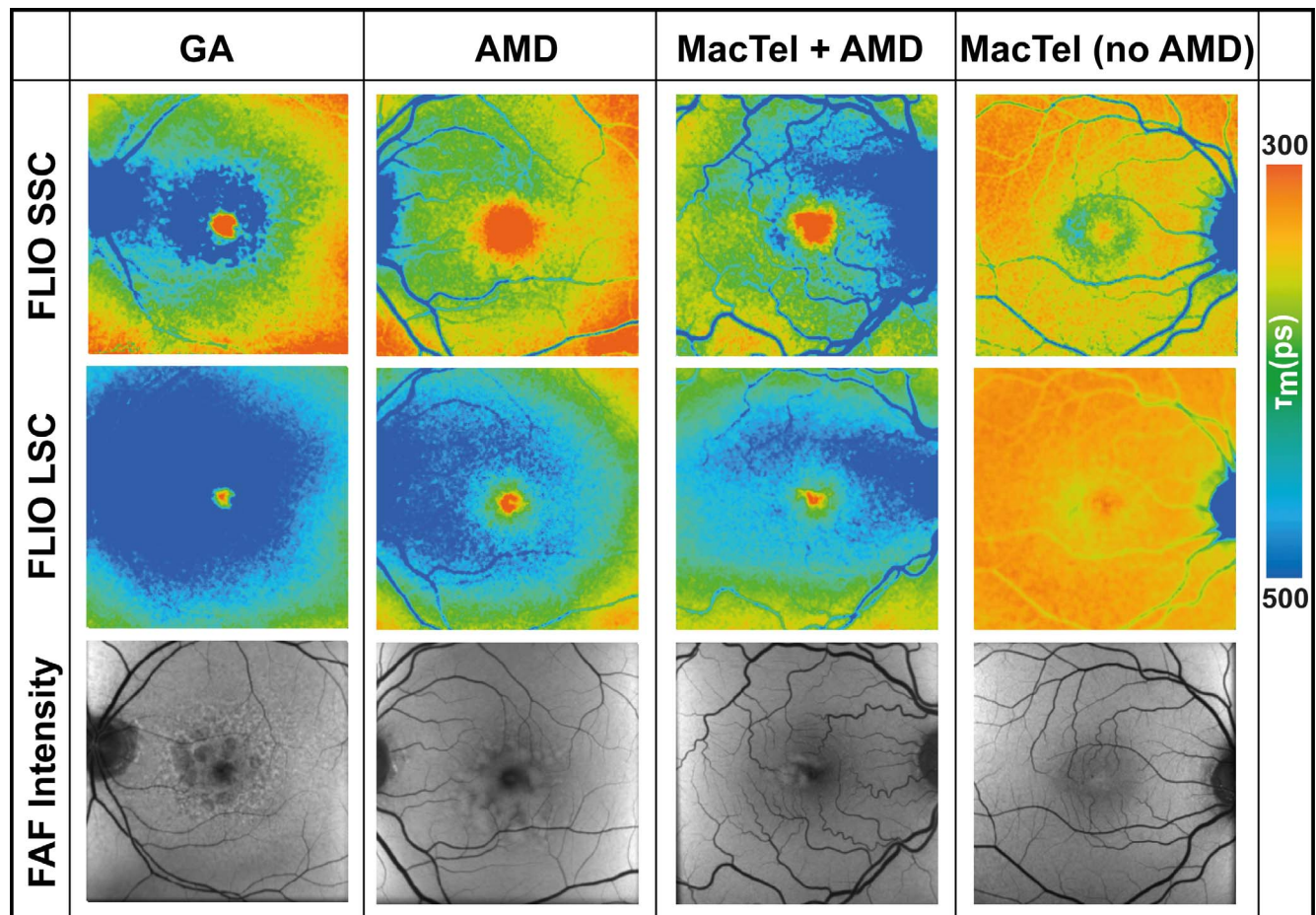


FIGURE 6. FAF lifetime (FLIO) images from both spectral channels, SSC (498–560 nm) and LSC (560–720 nm), as well as FAF intensity images from one patient with GA (m, 76 y), one patient with AMD (m, 68 y), one patient with AMD and MacTel (m, 71 y), and one patient with MacTel and no AMD (m, 61 y).

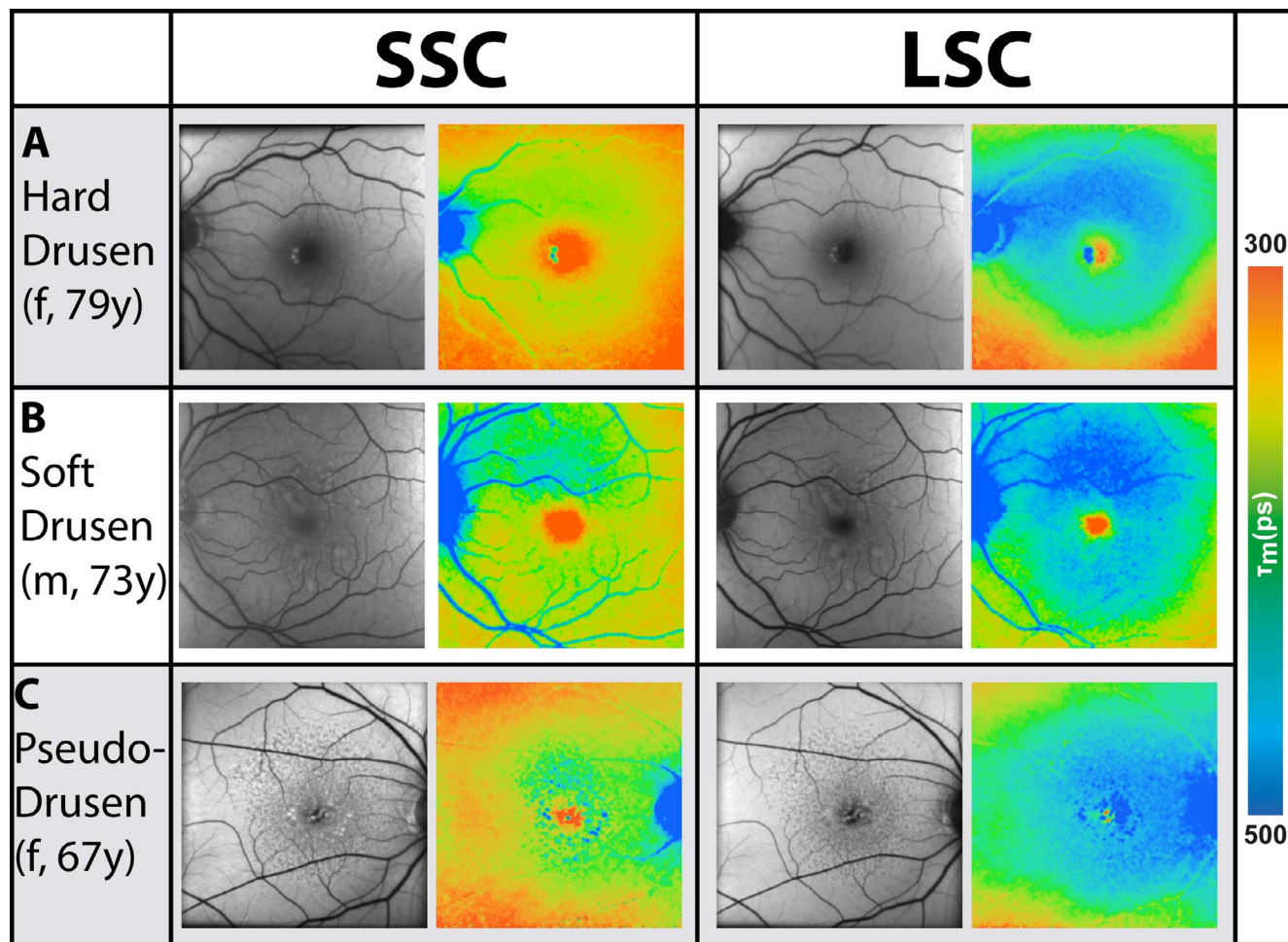


FIGURE 7. FAF intensity and lifetime images of three different patients with different types of drusen (A-C); the SSC (498–560 nm) and the LSC (560–720 nm) are shown.

corresponding retina without drusen (Table 4). The strongest significance was found for soft drusen.

Following the statistical method used in previous articles on drusen in FLIO,<sup>29</sup> we additionally performed an independent-sample *t*-test to compare mean FAF lifetimes of drusen with the adjacent retina without drusen. Here, only soft drusen showed significantly longer FAF lifetimes, and only in the LSC ( $P < 0.01$ ). Hard drusen ( $P = 0.089$ ) as well as pseudodrusen ( $P = 0.161$ ) only showed nonsignificant trends toward longer decays in the drusen.

Comparing different drusen types, no significant differences were found between hard drusen and pseudodrusen, as well as soft drusen and pseudodrusen. However, soft drusen appeared slightly more prolonged than hard drusen, which showed significance in the LSC ( $P < 0.05$ ).

## DISCUSSION

AMD is a vision-threatening disease, especially in its late forms. Metabolic changes may occur in early stages even before they are detectable with conventional imaging techniques.<sup>14</sup> This study hints that such metabolic alterations may be detectable with FLIO. Although treatment is available for exudative AMD, no sufficient treatments for early-stage AMD and/or end-stage GA have been developed thus far.<sup>34</sup> However, several clinical trials are in progress, and the approach targeting the

complement cascade seems promising.<sup>35</sup> Therefore, setting a focus on the diagnosis of AMD at very early stages is reasonable. Here, FLIO may be very helpful.

The principle of in vivo autofluorescence lifetime imaging at the retina was first introduced by Schweitzer and colleagues in 2002.<sup>36</sup> Since then, the method has been improved and investigated, and specific patterns were found for healthy eyes as well as retinal diseases.<sup>15–19,22,37</sup>

FAF lifetime patterns in healthy eyes have been thoroughly described in the literature.<sup>18,19,38</sup> Here, the fovea shows short FAF lifetimes caused by the fluorescence properties of the macular pigment carotenoids, which are especially visible within the SSC.<sup>18</sup> Intermediate-long FAF lifetimes are believed to be caused by lipofuscin and are homogeneously found across the entire retina; in macular holes they can be found inside the area of the hole.<sup>24</sup> The longest FAF lifetimes in healthy eyes are found at the area of the optic nerve.

Patterns of FAF lifetimes in early and intermediate AMD vary from those of healthy eyes, and recently a general prolongation of FAF lifetimes in patients with AMD has been found.<sup>29</sup> In the present study, we were able to show a very specific pattern that we found in all eyes affected with AMD: these eyes presented a ring-shaped prolongation of the intermediate mean FAF lifetimes within the macula, which is especially visible within the LSC. This pattern seems to be associated with specific pathophysiologic changes that occur in AMD. It is visible in very early stages of the disease and also in patients

who have AMD and other retinal diseases. However, color scales must be adjusted accordingly for the pattern to be visible. In our study, 300 to 500 ps seemed appropriate. Previous studies often depicted FLIO images on a scale of 200 to 1000 ps; with this range, the pattern is less obvious.

Although this is a cross-sectional study investigating patients at one time point only, we believe that the pattern is not a fixed feature of AMD but rather progresses with disease progression and progressing changes in the retina due to AMD. This assumption is because the pattern is significantly longer in eyes with more advanced disease stages. The pattern in some of our healthy eyes shows less intense forms. Follow-up investigations will give a better idea on the exact progression of the pattern.

In late AMD stages, this pattern is visible when the color is adjusted. GA in nonexudative AMD has previously been analyzed.<sup>25,39</sup> Mean FAF lifetimes of atrophic regions, delineated with the FLIMX software as described elsewhere,<sup>39</sup> were  $616 \pm 343$  ps in the SSC and  $615 \pm 154$  ps in the LSC, which were also markedly different from unaffected retina and demonstrated even more prolongation of FAF lifetimes in comparison. If the GA area is smaller than the typical AMD pattern of approximately  $20^\circ$ , this is visible around the edges of the atrophy. The pattern appears very prominent in GA, which is likely because the disease is at a very advanced stage. GA sometimes spares the fovea.<sup>40,41</sup> Foveal sparing has been described in conditions other than GA; a ring-shaped distribution of reticular drusen with sparing of the fovea has been identified.<sup>42</sup> In this context, a connection to the choroidal blood flow or photoreceptor distributions has been suggested.<sup>42</sup> We also agree that there may be some protective factor present within the foveal region. The pattern we see in FLIO images seems not to affect this region (especially in early stages of AMD), and we did not see significant differences at the fovea between AMD and healthy eyes. The mechanisms behind this still need to be further investigated.

We can only hypothesize in which retinal layer the observed FLIO changes may occur. The prolongation of  $\tau_m$  in the observed typical patterns for AMD appear strongest within the LSC. This finding suggests that the affected fluorophores must be ones with most of their fluorescence emission within this channel. It has previously been discussed that the prolongation of mean FAF lifetimes may be an early sign for the accumulation of bis-retinoids in the RPE,<sup>37</sup> which not only have intrinsic fluorescence but may also block relatively short autofluorescence from other fluorophores in the RPE and therefore result in prolonged FAF lifetimes in AMD.<sup>14,37</sup> Early FAF lifetime imaging studies have shown that the LSC is predominantly influenced by lipofuscin.<sup>16</sup> Additionally, more recent studies have also suggested that the intermediate-long  $\tau_m$  are associated with lipofuscin.<sup>24</sup> In AMD, these intermediate-long FAF lifetimes are shifted to longer means. A recent study by Dysli et al.<sup>29</sup> found general prolongations over the area of a standardized ETDRS grid. This shift to longer mean FAF lifetimes provides a hint that the lipofuscin composition may also change in early AMD, even before drusen can be found at the fundus. Alterations in lipofuscin content or character may interfere with the healthy retina.

The RPE is not the only potential source for autofluorescence lifetime changes in AMD. For example, sub-RPE basal laminar and basal linear deposits might be causative of the prolongation of FAF lifetimes and could reflect an increase of connective tissue due to remodeling processes at the level of the RPE-photoreceptor band.<sup>29,37</sup> Moreover, Spaide and Curcio<sup>43</sup> reported accumulations of poorly characterized debris in the subretinal space in AMD that correlate with clinically observed reticular pseudodrusen. The same group showed a spatial correlation of these subretinal deposits with

damage to the rods.<sup>44</sup> Given that FLIO, as currently implemented, is a noninvasive in vivo imaging technique, we can only speculate as to these correlations without further histologic and biochemical evidence.

We were able to exclude an influence of other retinal diseases, and furthermore, we were able to distinguish AMD from other diseases, such as MacTel. However, with respect to the group of presumably healthy subjects, we must say that the described pattern has been found in 36% of the healthy Utah subjects. Although there was no age difference between healthy eyes that did and did not show the pattern, we cannot exclude that this may be a natural effect caused by aging. However, as the number of eyes affected with AMD rises with age, so does the number of early-stage/high-risk. We assume that we have enrolled some presumably healthy subjects who will eventually develop AMD. Additionally, of the 16 presumably healthy eyes with the pattern, 8 eyes also showed a few small drusen. These drusen were  $<63 \mu\text{m}$ , and therefore these subjects were graded as healthy according to the Beckman classification. All of these eight eyes showed the described FLIO pattern. None of the healthy eyes without the pattern had any drusen. Additionally, a positive family history (AMD in first-degree family members) was common in subjects with the pattern. Therefore, we hypothesize that we may be able to detect at least a risk for the development of AMD based on this pattern, but longitudinal studies following up on this pattern and the disease progression related to it are necessary to support or negate this hypothesis.

Investigating drusen in AMD, we agree with Dysli and colleagues<sup>29</sup> that it is difficult to identify them with FLIO. Although drusen often prolong the mean FAF lifetimes, individual drusen do not always present themselves with high contrast in FLIO images. To characterize drusen, clinical fundus examination and other imaging modalities, such as OCT, FAF intensity imaging, and fundus photography, were indispensable. Nevertheless, we did observe that drusen in general significantly prolong FAF lifetimes. Especially soft drusen showed the strongest differences to the retina without drusen. The association of soft drusen with the development of GA in a subset of AMD patients may explain this finding.<sup>45</sup> In a previous study, a two-tailed *t*-test was used to compare drusen with the retina, but it is not clear whether this was paired or unpaired.<sup>29</sup> When we conducted unpaired *t*-tests on our data, the only significance we found was for soft drusen. When conducting paired-sample *t*-tests, however, all drusen types showed significantly longer FAF decays relative to the adjacent retina.

A second difference with the previous study lies within the occurrence of drusen with shortened FAF lifetimes. Although Dysli and colleagues<sup>29</sup> observed individual drusen with such shortened FAF lifetimes, we did not find this in our study. However, Dysli and coworkers<sup>29</sup> also included patients with exudative AMD (33% of their study population), whereas exudative AMD was an exclusion criterion in our study. In eyes with exudative AMD, we also observed short FAF lifetimes in the LSC (Sauer and Bernstein, unpublished data, 2018). This difference in the study population likely accounts for the differences in our results.

This study has some limitations. First the number of eyes, especially for the analysis of drusen, is still relatively small. The second limitation is the inclusion of subjects who show a different AMD stage in the fellow eye. The Jena recruitment group included only one eye from each subject, which did not allow for further analysis of stage comparison between eyes of the same subject. Although the typical AMD pattern in FLIO images was very consistent in our two cohorts from different institutions, subsequent validation studies would be an important step to assess the reproducibility of these findings.

Additionally, there are some differences between the two FLIO devices due to a different calibration method. Although we did not include any healthy subjects younger than 50, there was an age difference of 5.3 years between the statistically investigated groups of healthy and non-GA AMD eyes, which was statistically significant ( $P < 0.05$ ). Including eyes with GA as well results in an age difference of 6.7 years; however, these eyes were not statistically compared with each other. This age difference was due to the difficulty of recruiting healthy elderly patients from the Moran Eye Center clinic, but we did include healthy patients up to the age of 85 years. The FLIO differences we see between healthy and AMD eyes were very striking, and we do not think that they can solely be accounted for by age.

Recently, Dysli and colleagues<sup>29</sup> described a dependence of the FAF lifetimes in eyes with AMD on the lens status. Other FLIO-based studies did not find significant differences between natural lenses and IOLs.<sup>46</sup> Moreover, previous studies found no significant difference of lens status when investigating differences between ROIs.<sup>24</sup> In our study, we found a significant difference between the lens status only in the SSC; here eyes with IOLs showed FAF lifetimes that were approximately 80 ps shorter than eyes with a natural lens ( $P < 0.05$ ). However, there was no significant difference ( $P = 0.4$ ) between IOL and natural lenses for the “Difference (OR minus C)” in the SSC. No significant differences between IOL and natural lens were found in the LSC. Additionally, we focus on the specific pattern that is visible in all eyes, regardless of the lens status. Similarly, the differences between different regions, which we investigate, were independent of the lens status. As the specific pattern is visible with either lens status, the lens influence is negligible for this study.

In conclusion, this study describes patterns of FAF lifetimes in AMD, which have a characteristic ring-shaped prolongation of mean FAF lifetimes identified in distinct cohorts from two academic institutions. The FAF lifetime patterns can be found in early stages of the disease and may carry important prognostic ability as a very early predictor for patients at risk of developing AMD. We believe that this pattern may progress with disease progression, which needs to be investigated in longitudinal studies. This study also sheds light on an anatomical component to the FAF patterns in AMD, which was most often found to begin in the S-N side of the macula. Although we investigated these patterns for nonexudative AMD only, we strongly suspect that they may be detected in exudative AMD as well. This needs to be further investigated. Likewise, longitudinal studies are indispensable to prove a relation of this pattern to the development of AMD in healthy individuals who also exhibit this pattern. These promising findings in patterns of FAF lifetimes observed in early AMD represent an important step toward earlier identification, monitoring, and treatment of AMD.

### Acknowledgments

The authors thank Heidelberg Engineering for providing the FLIO as well as for their technical assistance, Yoshihiko Katayama, PhD, for his technical assistance, and Matthias Klemm, PhD, for providing the FLIMX software, and all colleagues from the John A. Moran Eye Center and the Sharon Eccles Steele Center for Translational Medicine who helped recruit and image the patients.

Supported in part by an unrestricted departmental grant from Research to Prevent Blindness and National Institutes of Health Grants EY11600 and EY14800.

Disclosure: **L. Sauer**, None; **R.H. Gensure**, None; **K.M. Andersen**, None; **L. Kreilkamp**, None; **G.S. Hageman**, Voyant Biotherapeutics, LLC (E, I, S), AGTC, Inc. (C); **M. Hammer**, None; **P.S. Bernstein**, None

### References

1. Klein R, Cruickshanks KJ, Nash SD, et al. The prevalence of age-related macular degeneration and associated risk factors. *Arch Ophthalmol*. 2010;128:750-758.
2. Klein R, Klein BE, Jensen SC, Meuer SM. The five-year incidence and progression of age-related maculopathy: the Beaver Dam Eye Study. *Ophthalmology*. 1997;104:7-21.
3. Friedman DS, O'Colmain BJ, Munoz B, et al. Prevalence of age-related macular degeneration in the United States. *Arch Ophthalmol*. 2004;122:564-572.
4. Gehrs KM, Anderson DH, Johnson LV, Hageman GS. Age-related macular degeneration—emerging pathogenetic and therapeutic concepts. *Ann Med*. 2006;38:450-471.
5. Hammond CJ, Webster AR, Snieder H, Bird AC, Gilbert CE, Spector TD. Genetic influence on early age-related maculopathy: a twin study. *Ophthalmology*. 2002;109:730-736.
6. Seddon JM, Ajani UA, Mitchell BD. Familial aggregation of age-related maculopathy. *Am J Ophthalmol*. 1997;123:199-206.
7. Meyers SM, Greene T, Gutman FA. A twin study of age-related macular degeneration. *Am J Ophthalmol*. 1995;120:757-766.
8. Gorusupudi A, Nelson K, Bernstein PS. The Age-Related Eye Disease 2 Study: micronutrients in the treatment of macular degeneration. *Adv Nutr*. 2017;8:40-53.
9. Bernstein PS, Li B, Vachali PP, et al. Lutein, zeaxanthin, and meso-zeaxanthin: the basic and clinical science underlying carotenoid-based nutritional interventions against ocular disease. *Prog Retin Eye Res*. 2016;50:34-66.
10. Hageman GS, Mullins RE. Molecular composition of drusen as related to substructural phenotype. *Mol Vis*. 1999;5:28.
11. Hageman GS, Luthert PJ, Victor Chong NH, Johnson LV, Anderson DH, Mullins RE. An integrated hypothesis that considers drusen as biomarkers of immune-mediated processes at the RPE-Bruch's membrane interface in aging and age-related macular degeneration. *Prog Retin Eye Res*. 2001;20:705-732.
12. Anderson DH, Radeke MJ, Gallo NB, et al. The pivotal role of the complement system in aging and age-related macular degeneration: hypothesis re-visited. *Prog Retin Eye Res*. 2010;29:95-112.
13. Anderson DH, Mullins RE, Hageman GS, Johnson LV. A role for local inflammation in the formation of drusen in the aging eye. *Am J Ophthalmol*. 2002;134:411-431.
14. Khan KN, Mahroo OA, Khan RS, et al. Differentiating drusen: drusen and drusen-like appearances associated with ageing, age-related macular degeneration, inherited eye disease and other pathological processes. *Prog Retin Eye Res*. 2016;53:70-106.
15. Schweitzer D. Metabolic mapping. In: Holz F, Spaide R, eds. *Medical Retina*. Berlin: Springer; 2010:107-123.
16. Schweitzer D, Schenke S, Hammer M, et al. Toward metabolic mapping of the human retina. *Microsc Res Tech*. 2007;70:410-419.
17. Schweitzer D, Hammer M, Schweitzer F, et al. In vivo measurement of time-resolved autofluorescence at the human fundus. *J Biomed Opt*. 2004;9:1214-1222.
18. Sauer L, Schweitzer D, Ramm L, Augsten R, Hammer M, Peters S. Impact of macular pigment on fundus autofluorescence lifetimes. *Invest Ophthalmol Vis Sci*. 2015;56:4668-4679.
19. Dysli C, Queller G, Abegg M, et al. Quantitative analysis of fluorescence lifetime measurements of the macula using the fluorescence lifetime imaging ophthalmoscope in healthy subjects. *Invest Ophthalmol Vis Sci*. 2014;55:2106-2113.
20. Klemm M, Dietzel A, Haueisen J, Nagel E, Hammer M, Schweitzer D. Repeatability of autofluorescence lifetime imaging at the human fundus in healthy volunteers. *Curr Eye Res*. 2013;38:793-801.

21. Dysli C, Berger L, Wolf S, Zinkernagel MS. Fundus autofluorescence lifetimes and central serous chorioretinopathy. *Retina*. 2017;37:2151-2161.
22. Sauer L, Gensure RH, Hammer M, Bernstein PS. Fluorescence lifetime imaging ophthalmoscopy (FLIO)—a novel way to assess macular telangiectasia type 2 (MacTel). *Ophthalmol Retina*. 2018;2:587-598.
23. Schmidt J, Peters S, Sauer L, et al. Fundus autofluorescence lifetimes are increased in non-proliferative diabetic retinopathy. *Acta Ophthalmol*. 2017;95:33-40.
24. Sauer L, Peters S, Schmidt J, et al. Monitoring macular pigment changes in macular holes using fluorescence lifetime imaging ophthalmoscopy (FLIO). *Acta Ophthalmol*. 2017;95:481-492.
25. Dysli C, Wolf S, Zinkernagel MS. Autofluorescence lifetimes in geographic atrophy in patients with age-related macular degeneration. *Invest Ophthalmol Vis Sci*. 2016;57:2479-2487.
26. Dysli C, Wolf S, Hatz K, Zinkernagel MS. Fluorescence lifetime imaging in Stargardt disease: potential marker for disease progression. *Invest Ophthalmol Vis Sci*. 2016;57:832-841.
27. Dysli C, Schurch K, Pascal E, Wolf S, Zinkernagel MS. Fundus autofluorescence lifetime patterns in retinitis pigmentosa. *Invest Ophthalmol Vis Sci*. 2018;59:1769-1778.
28. Andersen KM, Sauer L, Gensure RH, Hammer M, Bernstein PS. Characterization of retinitis pigmentosa using fluorescence lifetime imaging ophthalmoscopy (FLIO). *Trans Vis Sci Tech*. In press.
29. Dysli C, Fink R, Wolf S, Zinkernagel MS. Fluorescence lifetimes of drusen in age-related macular degeneration. *Invest Ophthalmol Vis Sci*. 2017;58:4856-4862.
30. Schweitzer D, Gaillard ER, Dillon J, et al. Time-resolved autofluorescence imaging of human donor retina tissue from donors with significant extramacular drusen. *Invest Ophthalmol Vis Sci*. 2012;53:3376-3386.
31. Ferris FL III, Wilkinson CP, Bird A, et al. Clinical classification of age-related macular degeneration. *Ophthalmology*. 2013; 120:844-851.
32. Becker W. *The bh TCSPC Handbook*. 6th ed. Berlin: Becker & Hickl GmbH; 2014.
33. Klemm M, Schweitzer D, Peters S, Sauer L, Hammer M, Hauelsen J. FLIMX: a software package to determine and analyze the fluorescence lifetime in time-resolved fluorescence data from the human eye. *PLoS One*. 2015;10: e0131640.
34. Taskintuna I, Elsayed ME, Schatz P. Update on clinical trials in dry age-related macular degeneration. *Middle East Afr J Ophthalmol*. 2016;23:13-26.
35. Boyer DS, Schmidt-Erfurth U, van Lookeren Campagne M, Henry EC, Brittain C. The pathophysiology of geographic atrophy secondary to age-related macular degeneration and the complement pathway as a therapeutic target. *Retina*. 2017;37:819-835.
36. Schweitzer D, Kolb A, Hammer M, Anders R. Time-correlated measurement of autofluorescence. A method to detect metabolic changes in the fundus [in German]. *Ophthalmologie*. 2002;99:774-779.
37. Dysli C, Wolf S, Berezin MY, Sauer L, Hammer M, Zinkernagel MS. Fluorescence lifetime imaging ophthalmoscopy. *Prog Retin Eye Res*. 2017;60:120-143.
38. Sauer L, Andersen KM, Li B, Gensure RH, Hammer M, Bernstein PS. Fluorescence lifetime imaging ophthalmoscopy (FLIO) of macular pigment. *Invest Ophthalmol Vis Sci*. 2018; 59:3094-3103.
39. Sauer L, Klemm M, Peters S, Schweitzer D, et al. Monitoring foveal sparing in geographic atrophy with fluorescence lifetime imaging—a novel approach. *Acta Ophthalmol*. 2017;96:257-266.
40. Maguire P, Vine AK. Geographic atrophy of the retinal pigment epithelium. *Am J Ophthalmol*. 1986;102:621-625.
41. Sarks JP, Sarks SH, Killingsworth MC. Evolution of geographic atrophy of the retinal pigment epithelium. *Eye*. 1988;2:552-577.
42. Steinberg JS, Fleckenstein M, Holz FG, Schmitz-Valckenberg S. Foveal sparing of reticular drusen in eyes with early and intermediate age-related macular degeneration. *Invest Ophthalmol Vis Sci*. 2015;56:4267-4274.
43. Spaide RF, Curcio CA. Drusen characterization with multimodal imaging. *Retina*. 2010;30:1441-1454.
44. Curcio CA, Messinger JD, Sloan KR, McGwin G, Medeiros NE, Spaide RF. Subretinal drusenoid deposits in non-neovascular age-related macular degeneration: morphology, prevalence, topography, and biogenesis model. *Retina*. 2013;33:265-276.
45. Smith RT, Chan JK, Busuoiu M, Sivagnanavel V, Bird AC, Chong NV. Autofluorescence characteristics of early, atrophic, and high-risk fellow eyes in age-related macular degeneration. *Invest Ophthalmol Vis Sci*. 2006;47:5495-5504.
46. Sauer L, Peters S, Schmidt J, et al. Monitoring macular pigment changes in macular holes using fluorescence lifetime imaging ophthalmoscopy. *Acta Ophthalmol*. 2017;95:481-492.